



## Open Archive Toulouse Archive Ouverte (OATAO)

OATAO is an open access repository that collects the work of some Toulouse researchers and makes it freely available over the web where possible.

This is an author's version published in: <https://oatao.univ-toulouse.fr/20967>

**Official URL:** <http://www.optro2018.com/proceedings2018/>

### To cite this version :

Canuet, Lucien and Lacan, Jérôme and Rissons, Angélique and Vedrenne, Nicolas and Artaud, Géraldine Cross layer optimisation for adaptive-optics corrected satellite to Ground laser links. (2018) In: 8th symposium on Optronics in Defence and Security - OPTRO2018, 6 February 2018 - 8 February 2018 (Paris, France).

Any correspondence concerning this service should be sent to the repository administrator:

[tech-oatao@listes-diff.inp-toulouse.fr](mailto:tech-oatao@listes-diff.inp-toulouse.fr)

# CROSS LAYER OPTIMISATION FOR ADAPTIVE-OPTICS CORRECTED SATELLITE-TO-GROUND LASER LINKS

L. Canuet<sup>(1,2,3,\*), J. Lacan<sup>(2), A. Rissons<sup>(2), N. Védrenne<sup>(3), G. Artaud<sup>(1)</sup></sup></sup></sup></sup>

<sup>(1)</sup> CNES, 18, av. Edouard Belin, 31401 Toulouse Cedex 9, France

<sup>(2)</sup> ISAE-Supaéro and TeSA, Toulouse, France

<sup>(3)</sup> ONERA, Theoretical and Applied Optics Department, 92322 Châtillon Cedex, France

\*Corresponding author : L. Canuet (email: lucien.canuet@onera.fr)

**KEYWORDS:** FSO Communications, adaptive-optics, satellite downlink, coding, interleaving

## ABSTRACT

For future satellite-to-ground communications link, very high throughput might be achievable at a reasonable cost assuming the use of existing single mode components developed for fiber technologies (optical detectors and amplifiers, MUX/DEMUX...). The influence of atmospheric turbulence degrades the injection efficiency of the incoming wave into single mode components. This leads to signal fading and channel impairments. Several mitigation strategies are considered to prevent them. The use of adaptive optics should contribute to reduce substantially the criticality of the fading at the expense of potentially complex and expensive systems if very high stability of the injection is requested. The use of appropriate numerical mitigation techniques (coding+interleaving) can help to relax the specifications and cost of AO systems but could lead among others to unmanageable buffer size. Thus the specification of AO correction and interleavers/forward error codes should be addressed jointly.

A model to evaluate the channel capacity in terms of outage probability and packet error rate has been developed that jointly takes into account partial correction by AO and channel interleaving. It includes the capability to evaluate coded transmission performance over the correlated FSO channel in satellite-to-ground scenarios.

This model is presented here and confronted to numerical simulations for several distinct correction cases. The interdependence of AO correction with numerical mitigation techniques is investigated.

## 1. INTRODUCTION

For future satellite-to-ground communications link, very high throughput might be achievable at a reasonable cost assuming the use of existing single mode components developed for fiber technologies such as erbium doped fiber amplifier (EDFA). However, atmospheric turbulence

degrades the injection efficiency of the incoming wave into single mode components. This leads to signal fading and channel impairments. Several mitigation strategies are considered to prevent them. The use of adaptive-optics (AO) should contribute to reduce substantially the severity of the fading at the expense of potentially complex and expensive systems if very high injection stability is required.

Therefore, to reduce the loss in useful information and to relax by the same way the specifications and cost of AO systems, numerical reliability mechanisms such as interleaving and coding techniques have to be considered. The latter introduce a degree of data redundancy, which allows a transmitted codeword to be correctly interpreted despite the loss of a significant fraction of the individual codeword elements. Nevertheless, they are usually adapted to combat randomly distributed errors rather than bursty errors that are characteristic of the free-space optical channel.

Such burst of errors are due to the typical correlation time of the FSO channel -milliseconds to fractions of milliseconds- and the usually envisaged data rates -several dozen Gbps- that induce fading events that can be much longer than several codewords. As depicted, in a simplified fashion, by the diagram presented in Fig. 1, this will inevitably results in an unrecoverable loss of information. To overcome this bursty distribution of errors, symbol interleaving is mandatory. Typically, these interleavers, after disassembling every codeword will spread their individual elements with a temporal interval comparable to a characteristic duration of the channel fades.

In addition to the latency inherently introduced by such a fading mitigation technique, the interleaving process may simply lead to very large memory sizes at the satellite end, hence potentially increasing the complexity and the cost of the system.

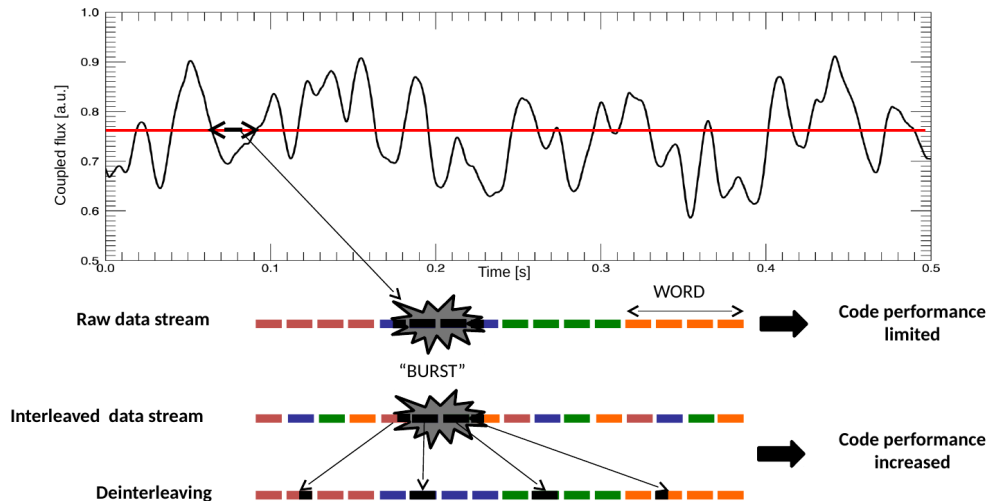


Figure 1. Illustration of the impact of the bursty nature of the FSO communication channel on the design of data reliability mechanisms such as interleaving and error coding codes.

Furthermore, it is likely that such satellite-to-ground downlinks will be implemented as part of global networks, such as the one presented in Fig. 2, and not solely as point-to-point transmissions. They will make use of optical data relay systems such as the European Data Relay System [1] and will require the implementation of optimized optical ground stations networks [2], deployable /transportable means such as High Altitude Platforms [3], and ground systems [4]. Similarly, but in the context of military applications, several network-centric operational concepts providing battlefield information using high capacity FSO links from an array of different assets (space, airborne or terrestrial) are investigated and/or under implementation [5,6,7]. For either civilian or military applications, such networks require the optimization of data reliability mechanisms not only at the physical layer (PL) but at the different layers of the communication stack. Indeed, on any correlated channel, by studying the interactions between these reliability mechanisms at different layers, cross-layering strategies that allow for better overall performances may be found. Extensive work on numerical approaches to mitigate free-space optical channel impairments were conducted in the US [8], Germany [9] and Japan [10]. Yet, very few results have been published on the advantages related to potential cross-layer allocation strategies of memory as well as redundancy.

Therefore, in order to appropriately and efficiently optimize such strategies in accordance with the typical evolution times of the channel -that are impacted by the ground-based AO correction performance- an accurate optimization of the overall system is required.

In that regard, the present paper emphasizes numerical results characterizing the coded performances of a communication system consisting of a combination of cross-layered data reliability mechanisms for satellite-to-ground laser links corrected by AO. In Section 2 we introduce a model that provides time series of single-mode-fiber (SMF) coupled flux fades after AO correction. The cross-layering strategy that we have adopted as well as the model describing the coded performance estimators are described in Section 3. These models are exploited in Section 4 where results regarding two distinct AO systems in a LEO downlink scenario are presented.

## 2. SINGLE-MODE FIBER COUPLED FLUX PARTIALLY CORRECTED BY ADAPTIVE-OPTICS

The SMF coupled flux is subjected to variations conditioned by the turbulent wave-front distortions, themselves characterized by phase aberrations as well as log-amplitude fluctuations (or scintillation). Adaptive optics consists in a closed-loop system composed of a deformable mirror, a wavefront sensor and a real-time computer (RTC) that can correct such phase aberrations in real-time.

Increasing the diameter of the receiver will tend to decrease the coupled flux fluctuations thanks to aperture averaging of the log-amplitude fluctuations. However this is done at the expense of a more demanding AO system needed to partially correct phase aberrations.

A Monte-Carlo based simulation tool that models both the influences of residual phase fluctuations

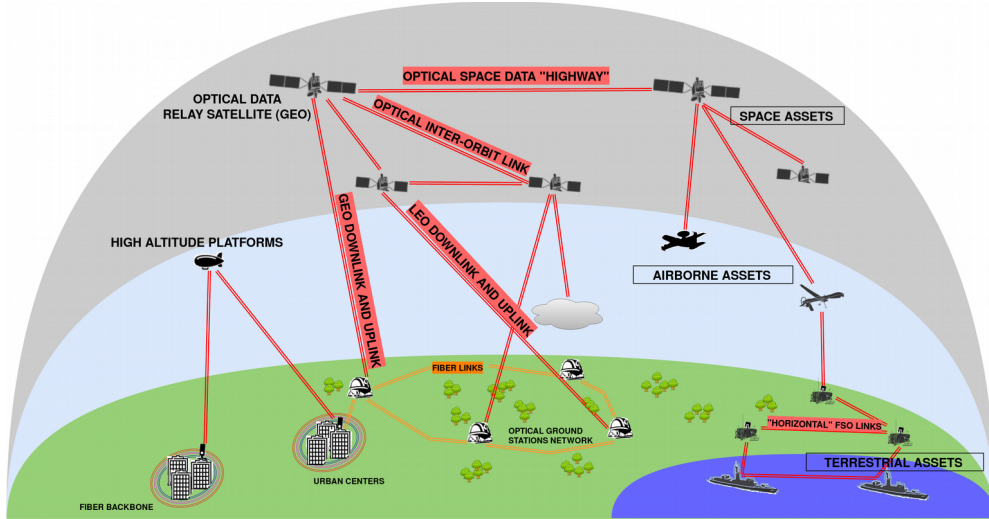


Figure 2. Hypothesized FSO network including satellite-to-ground optical links

and aperture averaged scintillation on the coupled flux has been used to generate the AO-corrected coupled flux attenuation time series used in the present paper. This simulation tool is based upon analytical models described in more details in [11]. It assumes statistical independence between scintillation and phase effects. This is soundly justified by considering the different origins of the fluctuations of the log-amplitude and the phase. The former are mostly caused by distant turbulence, whereas the latter are mostly introduced close to ground [12].

In order to generate partially corrected phase fluctuations this simplified simulator relies on the computation of random samples of centered normally distributed Zernike coefficients for describing the corrected phase. The temporal correlation of the latter is induced by filtering its temporal power spectra densities. The residual phase variance characterizing the performance of the simulated AO system includes terms related to the finite number of actuators (fitting error) of the deformable mirror. It also takes into account wave-front sensing precision (aliasing error) and, control-loop frequency (temporal error) that should not be neglected when considering transmission links from satellites with significant orbital velocities such as LEO-to-ground downlinks. However, because of the high optical power requested for high data rates (between 40 and 140 photons per bit [3]) and the typical timescale of evolution of the atmospheric turbulence, the influence of noise upon wave-front sensing is neglected.

Since it is widely accepted that the aperture-averaged irradiance fluctuations are log-normally distributed [13,14] as long as one does not consider strong log-amplitude fluctuation regimes,

random occurrences of the latter are obtained by generating centered normally distributed variables. Temporal correlations of the irradiance fluctuations are then induced by filtering in the Fourier domain. Finally, the AO corrected SMF coupled flux attenuation is therefore given by the product of an aperture-averaged scintillation term and a phase-related injection-losses term, assuming the independence between phase and log-amplitude fluctuations mentioned earlier.

Note that this simplified model has been compared to and validated by end-to-end simulations in [15] for the downlink scenarios presented here. It provides therefore an advantage over end-to-end simulations in terms of lower time and calculation resources needed when longer time series are required in order to accurately evaluate the performance of the system through the computation of telecommunication metrics such as packet-error rates (PER). Using the simplified simulator described above, time series of 8000 samples over a time horizon of 2 seconds were generated. The emphasis is put in this paper on the study of two LEO-to-ground scenarios characterized by two distinct AO systems: a "medium performance" and a "low performance" system.

Table 1. Characteristic link, turbulent and ao parameters of the LEO-to-ground downlink scenario

Downlink scenario	LEO
Elevation	20 deg
Range	1584 km
Orbital velocity	7.5 km/s
Rx aperture diameter	25 cm
Fried parameter	0.056 m
Log-ampl. variance	0.135

The turbulence and wind profiles of the simulated link are given in [11]. In Tab. 1, characteristic link as well as turbulent parameters common to both scenarios are summarized. The parameters of each AO system are given in Tab. 2.

Table 2.  
System parameters for the two AO systems

	High Perf. AO	Medium Perf. AO
# corrected radial orders	6	3
Control loop frequency	2 kHz	0.9 kHz
Residual phase variance	0.46 rad <sup>2</sup>	1.21 rad <sup>2</sup>
Average coupled flux attenuation	-3.2 dB	-5.1 dB

### 3. COMMUNICATION SYSTEM CROSS-LAYER PERFORMANCES EVALUATION

In order to improve the performance of satellite-to-ground optical transmissions, data reliability mechanisms at different levels of the communication stack can be explored. By exploiting the interactions between these reliability mechanisms at different layers, cross-layering techniques and strategies that allow for better overall performances can be implemented. As in a previously published paper [16] we investigate in the following a coding architecture consisting of an error correcting code (ECC) at the physical layer (PL) and an erasure code (EC) at higher layers (HL). It is represented by the diagram presented on Fig. 3. We consider as well the impact of interleaving at both the PL and the HL. By doing

so, arbitrarily small average decoded PER at the output of the HL can be obtained while limiting the sizes of the memories needed by the transmitter (satellite).

#### 3.1 Instantaneous Capacity Estimation at the Physical Layer

At the receiver PL, the transmission performance is characterized by the instantaneous channel capacity  $C(t)$  i.e. the maximum achievable data rate that can be reliably communicated between the transmitter and the receiver at a given instant  $t$ . Assuming soft decoding, the instantaneous capacity can be estimated using the mutual information between the detected electrical current -denoted  $y$  in the following- and the logical symbols sent  $x=\{\text{ZERO}, \text{ONE}\}$  as :

$$C(t) = \int \sum \Pr(x) f_{y|x}(y|x) \log_2 \left( \frac{f_{y|x}(y|x)}{\sum \Pr(x) f_{y|x}(y|x)} \right) dy \quad \text{Eq. 1}$$

where  $\Pr(x)$  is the probability of sending a ZERO or a ONE and is equal to 0.5. The probability distribution  $f_{y|x}(y|x)$  depends on the type of detector as well as the modulation considered. Assuming that, at the receiver the background illumination level is negligible, the emphasis is put here on an optically pre-amplified PIN detector using OOK modulation. The optical amplifier is mandatory in order to overcome the photodiode noise floor and improve the detection sensitivity. A single mode EDFA is considered here as the optical amplifier. The block diagram representing this receiver, as well as the whole PL (including AO) is given in Fig. 4.

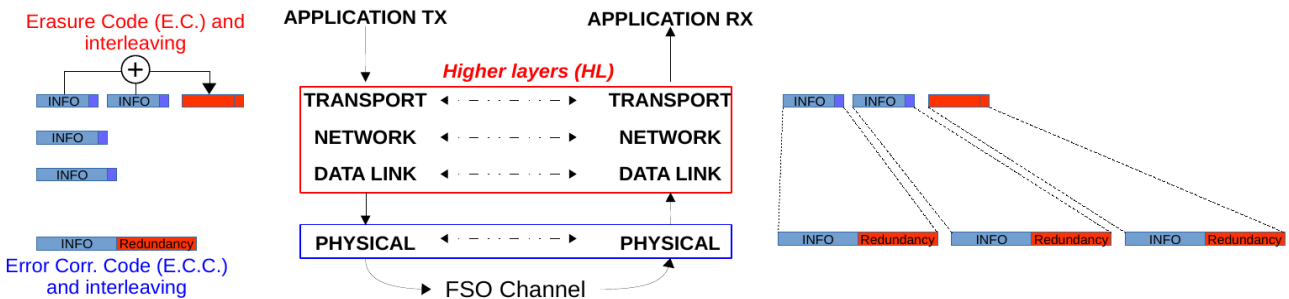


Figure 3. Diagram presenting the communication cross-layer architecture presented in this paper. The considered data reliability mechanisms consist of interleaving on both the physical and higher layers. Error correcting codes are used at the physical layer and erasure codes at the higher layers.

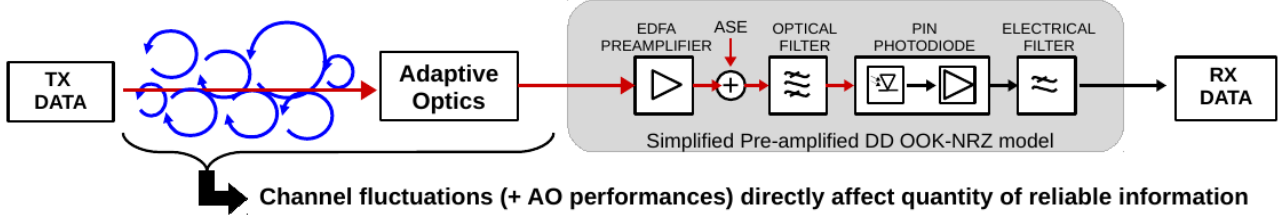


Figure 4. Physical layer and receiver/detection model block diagram.

After photo-detection, it is well known that the amplified spontaneous emission (ASE) induced by the EDFA generates in the electrical domain two additional beat noises referred to as signal-spontaneous and spontaneous-spontaneous beat noise. When moderately high amplifying gains are considered, the ASE noise dominates other sources of noise such as shot or thermal noises. In that case the probability density functions (PDF) of the electrical signal corresponding to either a logical ZERO or ONE have been theoretically shown to be non-Gaussian [17]. If a polarization filter is used at detection, a common approximation for such PDFs is given by [18]:

$$f_{y|x}(y|x=\text{ZERO}) = \frac{1}{\left(P_{\text{ASE}} R_s \frac{1}{M}\right)^M (M-1)!} \frac{y^{M-1}}{\exp\left(\frac{-y}{P_{\text{ASE}} R_s \frac{1}{M}}\right)} \quad \text{Eq. 2}$$

in the case of logical ZEROs, and by :

$$f_{y|x}(y|x=\text{ONE}) = \frac{1}{P_{\text{ASE}} R_s \frac{1}{M}} \left(\frac{y}{\bar{P}_1 R_s}\right)^{\frac{M-1}{2}} \exp\left(\frac{-y + \bar{P}_1 R_s}{P_{\text{ASE}} R_s \frac{1}{M}}\right) I_{M-1}\left(\frac{2\sqrt{y\bar{P}_1 R_s}}{P_{\text{ASE}} R_s \frac{1}{M}}\right) \quad \text{Eq. 3}$$

in the case of logical ONEs, and where  $R_s$ ,  $B_e$ ,  $B_o$ , correspond respectively to the detector responsivity, the double-sided electrical bandwidth of the receiver, the double-sided optical equivalent noise bandwidth of the filtered ASE and  $M=B_o/B_e$ . Note that generally these theoretical PDFs are valid in the case where  $B_e=1/T_s$  with  $T_s$  being the symbol period of the modulation considered. The time dependent output optical power of the signal is given by  $P_1(t) = P_{in}GA_{SMF}(t)$  where  $P_{in}$  is the average power coupled into the fiber and  $A_{SMF}(t)$  is the instantaneous attenuation of the AO corrected optical power coupled into the fiber. The ASE

power is given by  $P_{\text{ASE}}$  which depends on the inversion factor and the gain of the EDFA. The parameters corresponding to the pre-amplified detector presented in this paper are summarized in Tab. 3.

Table 3.  
Characteristic parameters of the detector

Transmission wavelength	1550 nm
Data rate	10 Gbps
Optical filter bandwidth	50 GHz
Electrical filter bandwidth	10 GHz
EDFA gain	30 dB
EDFA inversion factor	1
PIN responsivity	0.8 A/W

In practice, time series of instantaneous capacity are computed by applying Eq. 1, Eq. 2 and Eq. 3 to the times series of SMF coupled power attenuation generated by the simplified model described in Section 2. At the PL, to emulate the effect of a uniform convolutional interleaver at the transmitter and the associated de-interleaver at the receiver, the instantaneous channel capacity is uniformly averaged over a sliding window.

The PL memory needed at the transmitter in order to store the corresponding data is given by the product of the interleaver size in seconds and the data rate :

$$\text{Tx PL memory} = \text{PL interleaver size} \times \text{Data Rate}$$

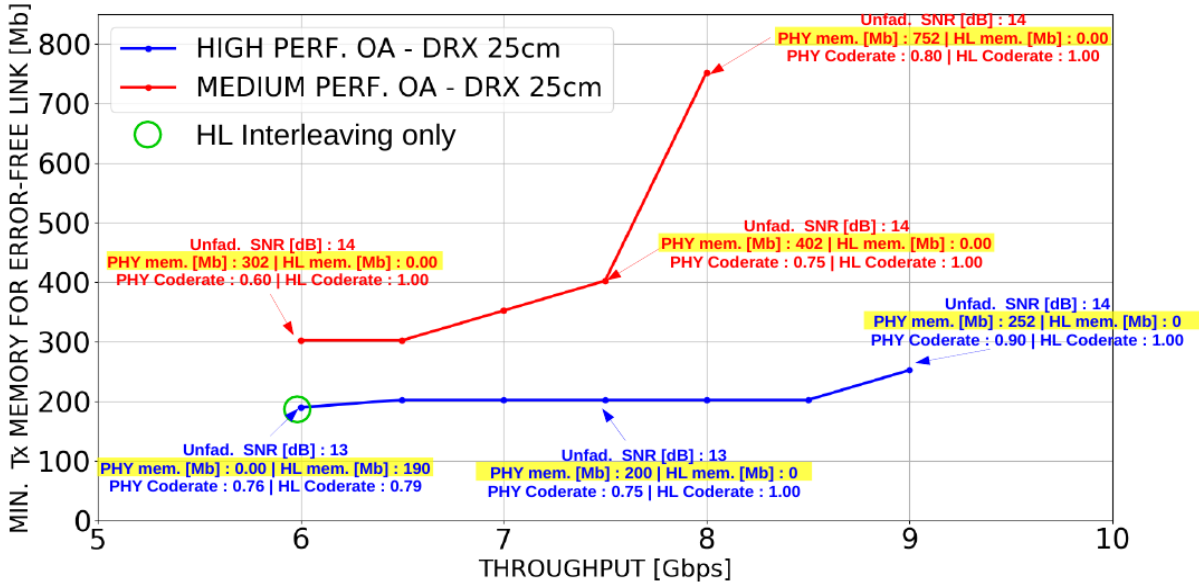


Figure 5. Evolution of the minimum total memory required by the transmitter in order to ensure an error-free transmission against the targeted throughput.

### 3.2 Instantaneous Packet-Error Rate Estimation at the Higher Layers

Let us assume that at the PL the transmitter sends information at a fixed coding rate (i.e. the proportion of the data-stream that is useful i.e. non-redundant) of  $R_o^{PL}$  bits/channel use. Moreover, let us consider a perfect (ECC) in the sense of Shannon's noisy channel coding theorem. This means that the decoding has an arbitrary small error probability as soon as the instantaneous channel capacity is greater than the coding rate. Because of the randomness of the propagation channel and therefore of the instantaneous channel capacity, there is a non-zero probability that  $C(t)$  is in outage i.e. falls under the code rate  $R_o^{PL}$ . When such an event occurs, the PL ECC in use will not allow for an "error-free" decoding. The erroneous packets are then erased. Therefore, the HL work on an input stream of instantaneous  $PER(t)$  that is the output of the PL. In practice, the instantaneous  $PER(t)$  at the output of the PL is obtained by thresholding the time series of instantaneous capacity to either a state of complete erasure (i.e.  $PER(t)=1$ ) when  $C(t)$  is in outage or to an error-free ECC decoding state (i.e.  $PER(t)=1$ ) otherwise.

At reception, prior to erasure decoding, the effect of packet convolutional interleaving/deinterleaving at the HL can be emulated again by a uniform sliding average window that slides over the time series of  $PER(t)$ , thus yielding a time series of interleaved HL PER denoted  $PER_{HL}^{intl.}(t)$  in the following. It is assumed that the coded packet of a given erasure codeword are spread over the

interleaver length. The product of the HL interleaver size with the data rate and the physical layer code rate  $R_o^{PL}$  yields the size of the HL memory needed at the transmitter in order to store the corresponding data:

$$\text{Tx HL memory} = \text{HL interleaver Size} \times \text{Data Rate} \times R_o^{PL}$$

After deinterleaving at the HL, the EC is assumed to be maximum distance separable. This means that the decoding is successful as soon as  $1 - PER_{HL}^{intl.}(t)$  is greater than  $R_o^{HL}$ , with  $R_o^{HL}$  denoting the EC rate. In that case, the instantaneous decoded PER at the HL output, denoted  $PER_{HL}^{dec.}(t)$ , is equal to zero. When  $PER_{HL}^{intl.}(t)$  is lower than the EC rate, the decoder fails and  $PER_{HL}^{dec.}(t) = PER_{HL}^{intl.}(t)$ .

### 4. NUMERICAL OPTIMIZATION AND RESULTS

As a final performance metric, we introduce the average of the instantaneous higher layer decoded PER, denoted  $E[PER_{HL}^{dec.}(t)]$  in the following. A transmission is considered error-free as soon as the condition  $E[PER_{HL}^{dec.}(t)]=0$  is met. Moreover, let us define the global code rate of the system as the product of the PL and HL code rates:

$$R_o^{GLOBAL} = R_o^{PL} R_o^{HL} \quad \text{Eq. 4}$$

This global code rate sets the throughput (i.e. the useful information rate) of the transmission when it is multiplied by the gross data rate (constant and fixed to 10 Gbps here, see Tab. 3. Note that the physical layer's code rate cannot be lower than the

global code rate.

The overall system under study presents numerous objective variables that can potentially be optimized over constrained ranges of several distinct parameters. As an objective variable, we focus hereafter on the minimum total memory required for an error-free downlink. That is, we have searched for the minimums  $Tx\_min\_memory = \min(Tx\_HL\ memory + Tx\_PL\ memory)$  at the transmitter allowing for  $E[PER_{HL}^{dec}(t)]$ . Such an optimization was conducted for several throughput ranging from 6 to 9 Gbps (i.e. for global code rates ranging from 0.6 to 0.9). Arbitrary constraints were put on the average required unfaded SNR (defined as  $P_{in}G/P_{ASE}$ ) and, the PL interleaver Sizes and HL interleaver Sizes. The former was allowed to range from 8 to 14 dB. The maximum interleavers sizes allowed were set to 0.375 s for both the PL and HL.

Fig. 5 shows the evolution of minimum required memory for an error-free transmission,  $Tx\_min\_memory$ , against the throughput for the both AO systems (see Tab. 2). For some points of interest on these curves, are reported the corresponding: required unfaded SNR, distribution of PL and HL code rates as well as PL and HL memories.

These results show unsurprisingly that targeting higher throughputs requires greater interleaving buffer memory as well as power (SNR). Furthermore, it is observed that compared to the medium performance system, the high performance AO system permits on average roughly a decrease of 80% of the required memory for every throughputs. Moreover, for the medium performance AO system, for every throughput considered, the minimum required memory is found for the highest SNR allowed. The use of a better performance AO can therefore lead to significant gains in terms of memory as well as required power from the satellite.

Interleaving on the PL is intrinsically more efficient than its HL counterpart which explains the fact that for every point except one the optimums correspond to interleavers exclusively allocated to the PL with no redundancy implemented at the HL (i.e.  $R_o^{PL}=R_o^{GLOBAL}$ ). Nevertheless, in less challenging transmissions conditions, that means lower throughput, high SNR and less channel fluctuations (better AO system), it was found that interleaving should be done exclusively on the HL. In the results presented here, such a case corresponds to the point, circled in green, characteristic of 6 Gbps throughput downlink using the high performance AO system. It is achieved for an optimum allocation of redundancy between the

PL error-correcting code and the HL erasure code.

Assuming that one aims to minimize the overall memory resources required by the system, these results highlight mainly two features. When facing challenging turbulent conditions, the global redundancy as well as the memory of the system should be distributed exclusively to the PL. When the turbulent conditions are less severe or their impact sufficiently reduced by AO it might be more advantageous to use only HL interleaving while considering an optimum cross-layer coding scheme. The case study presented in this paper highlight the impact of using an optimized AO correction on the overall system design of satellite-to-ground links and the relevance of studying such cross-layer interactions. For instance, PL interleaving usually requires dedicated hardware whereas the memory allocated to HL interleaving can be in practice implemented digitally using for instance the Tx's RAM (random-access memory) which is generally not exclusively meant for that purpose. This can potentially lead to a decrease in implementation complexity that is of interest especially at the satellite's end.

## 5. CONCLUSION

In this paper, simulation modeling and results assessing the performance of LEO-to-ground laser transmissions using adaptive optics in the framework of a cross-layer approach to the communication system are presented. The impact of AO correction combined with a cross-layer optimization of numerical reliability mechanisms including physical layer error correcting codes, higher layer erasure code and interleaving at both layers has been exposed. It is shown that by exploiting the interactions between these distinct reliability mechanisms better overall performance can be achieved. In particular, the global data memory required by the interleavers at the satellite end can be minimized while providing an error-free transmission. Finally, in addition to drastically reducing the aforementioned memories, it is shown that the use of better AO systems can have an impact on the optimal distribution of redundancy and interleaving memory over the physical and higher layers.

## ACKNOWLEDGMENT

This work was conducted in the framework of a Ph.D. thesis supervised by ISAE-Supaéro and ONERA, and co-funded by CNES, Airbus Defense and Space and Thales Alenia Space.

## REFERENCES

- [1] F. Heine, G. Mühlwinkel, H. Zech, S. Philipp-May



- and R. Meyer, "The European Data Relay System, high speed laser based data links," *2014 7th Advanced Satellite Multimedia Systems Conference and the 13th Signal Processing for Space Communications Workshop (ASMS/SPSC)*, Livorno, 2014, pp. 284-286. doi: 10.1109/ASMS-SPSC.2014.6934556
- [2] C. Fuchs and F. Moll, "Ground station network optimization for space-to-ground optical communication links," in *IEEE/OSA Journal of Optical Communications and Networking*, vol. 7, no. 12, pp. 1148-1159, Dec. 2015. doi: 10.1364/JOCN.7.001148
- [3] F. Fidler, M. Knappek, J. Horwath and W. R. Leeb, "Optical Communications for High-Altitude Platforms," in *IEEE Journal of Selected Topics in Quantum Electronics*, vol. 16, no. 5, pp. 1058-1070, Sept.-Oct. 2010. doi: 10.1109/JSTQE.2010.2047382
- [4] Karen Saucke, Christoph Seiter, Frank Heine, Mark Gregory, Daniel Tröndle, Edgar Fischer, Thomas Berkefeld, Mikael Feriencik, Marco Feriencik, Ines Richter, Rolf Meyer, "The Tesat transportable adaptive optical ground station," *Proc. SPIE 9739, Free-Space Laser Communication and Atmospheric Propagation XXVIII*, 973906 (15 March 2016);
- [5] J. C. Juarez, A. Dwivedi, A. R. Hammons, S. D. Jones, V. Weerackody and R. A. Nichols, "Free-Space Optical Communications for Next-generation Military Networks," in *IEEE Communications Magazine*, vol. 44, no. 11, pp. 46-51, November 2006. doi: 10.1109/MCOM.2006.248164
- [6] D. Voce, D.S. Gokhale, R. David, P. Bose, Considerations for a tsat quality of service architecture, in: *Proceedings of the Military Communications Conference (MILCOM) 2004*, Monterey, CA, Oct./Nov. 2004, pp. 85–92.
- [7] M. Gangl, D. Fisher, J. Zimmermann, L. Durham, "Airborne laser communication terminal for intelligence, surveillance and reconnaissance", in: *Proceedings of the SPIE Free-Space Laser Communications IV*, Denver, CO, Aug. 2004, pp. 92–103.
- [8] X. Zhu and J.M. Kahn, "Performance bounds for coded free-space optical communications through atmospheric turbulence channels," *IEEE Transactions on communications*, Vol. 51, No. 8, August 2003.
- [9] Henniger, Hennes, "Packet-Layer Forward Error Correction Coding for Fading Mitigation," In: *Proceedings of SPIE – Volume 6304*, 630419-1-630419-8. SPIE Optical Press. Free-Space Laser Communications VI, 2006-08-15 -2006-08-17, San Diego, California, USA. ISBN 0-8194-6383-3. ISSN 0277-786X.
- [10] Takenaka, H., Okamoto, E., and Toyoshima, M., "Low-density generator matrix code for correcting errors with a small optical transponder," In *IEEE International Conference on Space Optical Systems and Applications*, 2015, pp. 1-4.
- [11] N. Vedrenne and J.-M. Conan and C. Petit and V. Michau, "Adaptive optics for high data rate satellite to ground laser link," In *Proc. SPIE 9739, Free-Space Laser Communication and Atmospheric Propagation XXVIII*, 97390E, 2016
- [12] N. Perlot, "Turbulence-induced fading probability in coherent optical communication through the atmosphere," *Appl. Opt.*, 29, pp 7218–7226, OSA, vol.46, October 2007.
- [13] Tatarski, V.I., *Wave Propagation In a Turbulent Medium*, Dover Publications, Inc. New York, 1961.
- [14] Strohbehn, J. W., *Laser Beam Propagation in the Atmosphere*, Springer Berlin Heidelberg, 1978.
- [15] L. Canuet, N. Védrenne, J-M. Conan, C. Petit, G. Artaud, A. Rissons, and J. Lacan "Statistical properties of single-mode fiber coupling of satellite-to-ground laser links partially corrected by adaptive optics," accepted for publication in *JOSA A*.
- [16] Canuet Lucien, Lacan Jérôme, Védrenne Nicolas, Géraldine Artaud, and Rissons Angélique, "Performance Evaluation of Coded Transmission for Adaptive-Optics Corrected Satellite-To-Ground Laser Links", in *proceedings of ICSOS (IEEE International Conference on Space Optical Systems and Applications)*, November 2017 – Naha, Okinawa, Japan
- [17] P. A. Humblet and M. Azizoglu, "On the bit error rate of lightwave systems with optical amplifiers," in *Journal of Lightwave Technology*, vol. 9, no. 11, pp. 1576-1582, Nov 1991.
- [18] B. Chan and J. Conradi, "On the non-Gaussian noise in erbium-doped fiber amplifiers," in *Journal of Lightwave Technology*, vol. 15, no. 4, pp. 680-687, Apr 1997.